Chapter

Evaluation Methods of Mechanical Properties of Micro-Sized Specimens

Takashi Nagoshi, Tso-Fu Mark Chang

Abstract

Micro-sized components have been widely used to microelectromechanical systems (MEMSs) and medical apparatus in recent years. Measurement methodologies of the mechanical property of small materials need to be improved for structural designing of these devices because of their component size reduced to micro- or nano-regime where sample size effects emerge. Mechanical properties and deformation behavior could be very different with their dimensions and geometries especially for small materials. Our experiments on the micro-specimen tested in different dimensions and loading directions are suitable for the evaluations of materials for MEMS components. In this chapter, recent studies on micro-testing of bending, compression, and tension with micro-sized samples will be presented including fabrication methods of non-tapered micro-sized specimens.

Keywords: micro-testing, strength, anisotropy, microstructure, electrodeposition

1. Introduction

1.1 Micro-testing

Micro-sized components have been used in microelectromechanical systems (MEMSs). Recent developments of MEMS are outstandingly fast and need improved performance, reliable Device lifetime, and Miniaturization. MEMSs are often made up of components below 10 μm in size. For example, MEMS-based accelerometers or gyroscopes were widely used in smartphones, gaming consoles, and location-based devices. Some more examples shown in **Figure 1** are optical switch (a), gyro sensor (b), and micro-windmill (c) [1]. Micro-components used in MEMS such as micro-spring, bending beams, and structural support of MEMS suffer from mechanical straining and need suitable mechanical properties. However, at these size scales, the classical physics are not always useful. Sample size effect, which will be described in later section, emerges. Thus, the micro-testing method with specimen whose sample size is in the same scales with actual MEMS components is needed.

Besides testing methods for small materials, micro-sized testing of each representative elementary volume in heterogeneous materials is of great interest. According to the Japanese Industrial Standards, material mechanical property evaluation requires samples with gauge length larger than the 10 mm for tensile, bend, and compression testing. These samples could include all representative

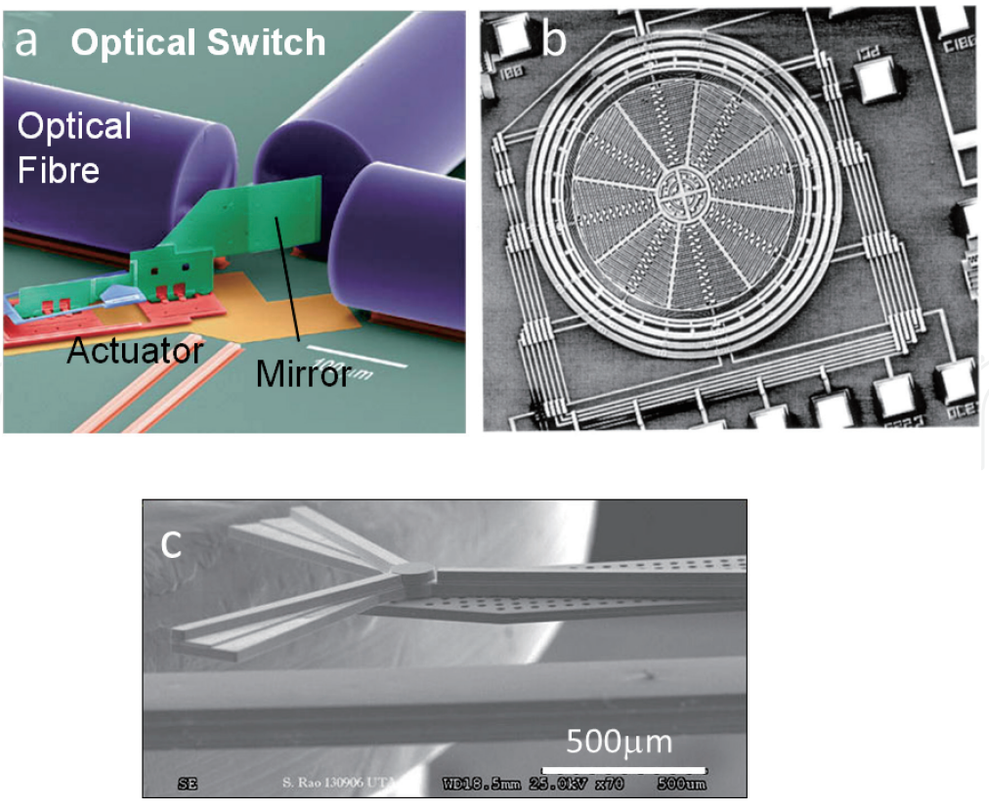

Figure 1.
Examples of MEMS devises: (a) optical switch, (b) gyro sensor, and (c) micro-windmill.

volume elements of materials, and thus the measurement results represent average properties of the material. On the other hand, micro-sized testing using micro-sized specimen can evaluate local mechanical properties such as second phase, locally damaged materials, and the interface or transition area among them.

1.2 Sample size effect

Mechanical property evaluations of small materials such as deposited film, heavily deformed metals, treated surface layer, etc. had been frequently conducted with indentation method because the size of the specimen can be very small and can easily conduct multiple tests for averaging. Hardness obtained from the indentation that repeatedly shows increase with decreasing indentation depth demonstrates a strong size effect [2–4]. Materials under the sharp indenter suffered from severe plastic flow from an early stage of indentation; thus, the deformations via dislocation and expansion of stacking faults are complicated, and strains had gradients from indentation site. The strain gradient under the indenter is supposed to be the main reason of indentation size effect as explained by strain gradient plasticity, which also justifies size effect on bending or torsional strength [4]. In an evolution of geometrical necessary dislocations with the presence of strain gradient, these formations induce an additional dislocations and cause material hardening, as supposed by Ashby [5]. Testing through compression or tension where strain gradients are absent had been conducted. Non-tapered pillar, i.e., no strain gradient inside, was fabricated and observed a generally unexpected size-dependent compression strength by Dimiduk et al. [6]. The following researches consistently showed size-dependent strength for tension and compression on various single-crystalline metals [7–11]. Size-dependent mechanisms on single-crystalline metals can be explained by the movement or evolution of dislocations in a limited volume of the small sample. Two commonly accepted models, dislocation starvation and source truncation, were proposed [12–14]. Dislocation starved condition observed by in-situ TEM

straining where new dislocation source nucleation needed with high stress [12, 15]. Truncated dislocations are observed as single-arm source where one end of the dislocation was pinned inside the specimens, and the other runs on the surface to attain strains [16]. These dislocation dynamics had been simulated using 3D discrete dislocation dynamics [17]. Size effects in single crystals had been well clarified based on the aforementioned dislocation mechanisms. However, size effects for the other deformations without dislocation motion such as grain boundary sliding and shear banding, which are frequently observed in nanocrystalline materials [18], are not yet been commonly understood. Rinaldi et al. [19] and Jang and Greer [20] have investigated the sample size effect on nickel nanocrystalline nano-pillars. They got different results: Jang and Greer observed a "smaller is weaker" dependence with the exponent smaller than one for single-crystalline metals, while Rinaldi et al. got very scattered result, which exhibits the slight increase in strength with decreasing sample size. Thus, sample size effect on nanocrystalline materials is inconclusive so far. Sample size effect on polycrystalline pillar has great interest in industries owing to miniaturization of MEMS devices reaching to its component scales at submicron or nano-regime.

1.3 Fabrications of MEMS

Metallic film formations are important processes for MEMS fabrication. There are two large classifications for film formation: one is the dry process and the other is the wet process. Dry process utilizes gas or metallic vapor for depositing metallic films on the surface of interest. Although it is a simple process, deposition rate is only sub-nm to several nm in a second [21, 22] and not suitable for industrial applications. On the other hand, one of the wet processes, electroplating, has been used for industrial fabrications of MEMS including components that require mechanical support thanks to fast deposition rate and controllable mechanical properties [23, 24].

The miniaturization of MEMS and IC goes into the nanoscale regime, the so-called nanotechnology. Each component size or wire width reaches several tens of nanometers. For the fabrication of such nanomaterials, gaps with an inversed geometry are filled with metals by deposition. In the gap filling, some problems happen as schematically shown in **Figure 2**. A liquid solution with surface tension and bad wettability to substrate do sometimes not fill the gaps or hydrogen gas bubbles evolved in the reaction. The areas without electrolyte were left unfilled during deposition leaving voids and pinholes [25]. We have developed a novel electroplating method with supercritical CO_2 emulsion (ESCE) to accomplish a successful metal gap fill [26, 27]. Emulsified

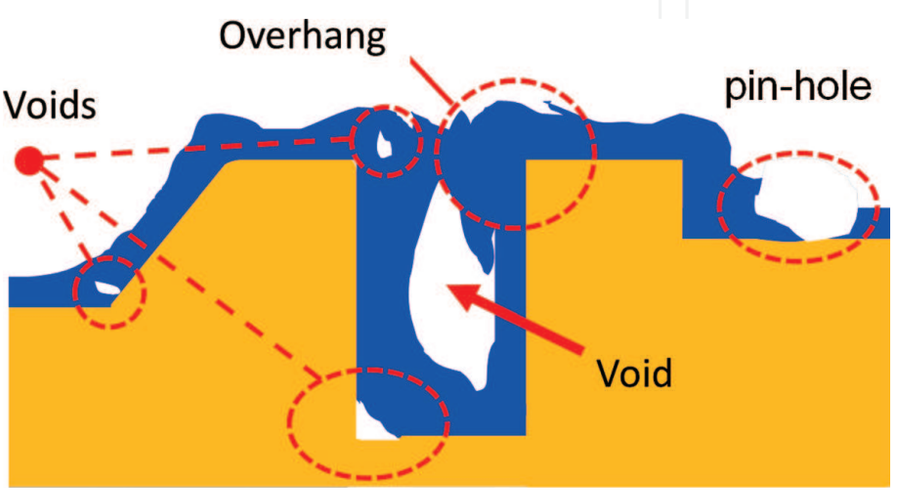

Figure 2.
Typical failures found in filling of gaps with electrodeposition.

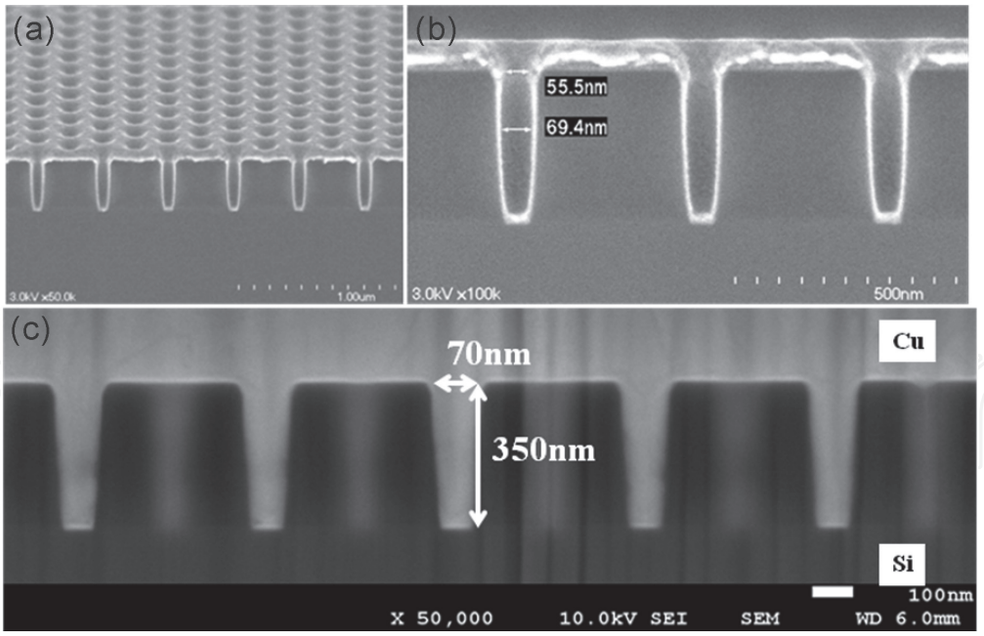

Figure 3.
Cross-sectional SEM images of (a) substrate with holes of 70 nm in diameter with aspect ratio of 5, (b) expanded image of (a), and (c) substrate filled with Cu electroplated in ESCE.

supercritical CO_2 with surfactant forms micelles which continuously bounce on the surface of cathode. Evolved hydrogen bubbles and unfilled gaps are removed by the micelles, and the deposition stopped at the bounced area. The deposition resumed with refreshed electrolyte which enhances local plating rate. These plating mechanisms are called periodic plating characteristics (PPC) [28, 29]. The efficient hole filling was observed in the Cu filling to the hole with 70 nm in diameter and 350 nm in depth as shown in **Figure 3** [30, 31]. PPC also contributes to the film strengthening via grain refinement. Strengthening of MEMS components is essential for further miniaturization and high reliability of the devices. However, the size effect discussed in the last section is aggressively studied for single-crystalline metals and only few researches on structured materials such as nanocrystalline metals.

2. Micro-pillar compression testing

2.1 Pillar fabrications

Compressions of fabricated pillar could be the most frequently employed testing method for small materials. Starting from a notable work by Uchic et al. [32] who first probe the size effect without stress gradient, numerous works had been done by micro-compression. Uchic et al. fabricated fascinating cylindrical micro-pillars by focused ion beam (FIB) from single-crystal Ni. Automated fabrications by a series of side-wall milling and rotation for tilted pillars enabled non-tapered cylindrical pillar fabrication, while most of the FIB fabrication uses single-direction milling; thus, pillar tapered inheriting a tilted milling wall in a FIB fabrication. We have proposed novel method to fabricate non-tapered pillars using conventional FIB only. Schematic images of fabrication process are shown in **Figure 4**. Multidirectional ion beam irradiation was utilized to eliminate tapering. The fabrication can be divided in three parts: (1) coarse milling, (2) tilted milling, and (3) finishing. Before FIB milling, samples were thinned down to approximately 50 mm and mounted with projected part on the sample holder. In (1) coarse milling, the tip of projected part milled to form a rectangle pillar with specimen thickness on

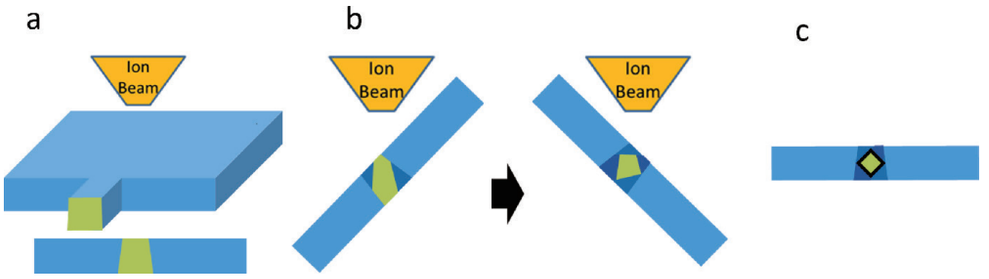

Figure 4.
Schematic images of process for compression pillar fabrication: (a) coarse milling, (b) tilted milling, and (c) finishing.

side length. Following (2) tilted milling, specimen tilted to ±45°; as more practically, sample rotated to 180° with tilting of 45°. The pillar size was reduced to a desired dimension leaving margins for finish milling. Tilted milling wall in FIB for this fabrication method results in a diamond-shaped cross section, which will be further modified in (3) finish milling. Using small current ion beam to minimize ion bombardment damage, the sample was milled from additional ±2.3° for each side of the pillar, i.e., ±47.3 and ±42.7 for four sides. SEM image of the fabricated pillar is shown in **Figure 5**. Uniform, non-tapered pillar is essential for the small-scale testing to reduce error in measurement. Finite element method indicates the tapering with the value of 20:1 (i.e., the angle between the post wall and the post axis is ~2.86°) results in the increase of yield strength and observed work hardening even the perfectly plastically deformed model used [33].

2.2 Compression test of electrodeposited nickel

Electrodeposition of metals can be used as fabrications of mechanical support of MEMS devices which will suffer from bending, compression, and tension from any directions. The anisotropic features of deposited metals arising from the

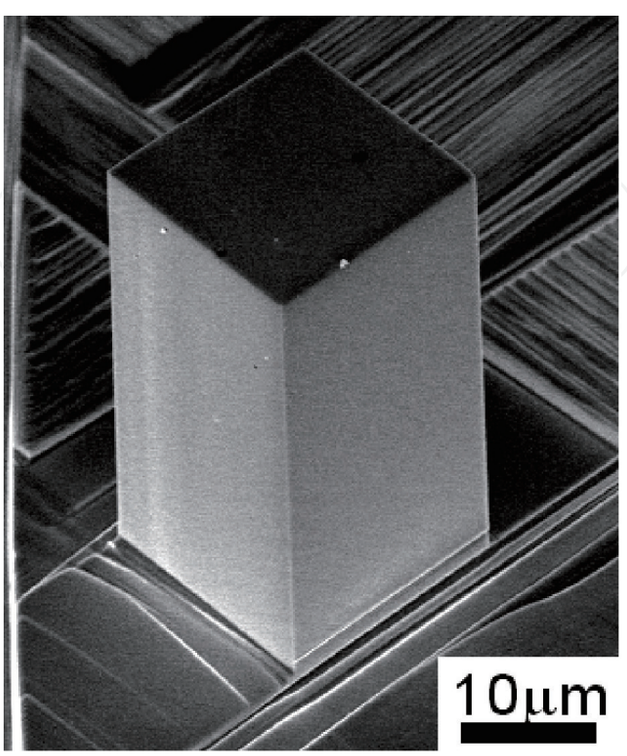

Figure 5.
Fabricated compression pillar made from single-crystalline nickel.

microstructures and orientations could strongly effect on the mechanical properties of the components. To evaluate the anisotropic characteristics and resulting reliability of MEMS devices, compression test on electrodeposited nickel was conducted.

Microstructures of Ni electrodeposited by additive-free Watt's bath are investigated. The substrate was film of pure Cu annealed at 673 K for 1 h in vacuum. The film's cross section was evaluated by the scanning electron microscope (SEM) equipped with an electron backscatter diffraction (EBSD) pattern detector. Orientation map overlaid with grain boundary map where Σ3 boundaries are colored yellow shown in **Figure 6** indicates fine columnar grains with diameter of around 100–200 nm grown toward film surface. Most of the columnar grain walls are Σ3 boundaries, corresponding to twin boundaries, although the stacking fault energy of Ni is relatively high [34]. High density of twins, 42% among high-angle grain boundaries observed in this film, which commonly observed in various kinds of electrodeposited metals [35–37].

Mechanical properties of Ni film electrodeposited in conventional Watt's bath were evaluated using micro-compression. Compression pillars were fabricated by the FIB milling method mentioned in the previous section. Two pillars with 20 × 20 × 40 μm were fabricated with pillar axis parallel and perpendicular to growth direction as shown in **Figure 7**. The compression test was conducted by indenting the pillar using flat-ended diamond indenter. Stress-strain curve in **Figure 8** shows increase in compressive stress of the parallel pillar. However, in the cantilever bending test of same material indicate maximum stress of 2080 and 1582 MPa for the parallel and perpendicular cantilever with respect to the growth direction [38], i.e., the strength increased when the load direction vertical to the growth direction of the electrodeposited film which is the opposite result than the compression test. This is related to the stress gradient present in bending test where the stress maximizes at a fixed end and decreases along beam direction or neutralizes at the center of beam. These results that imply the mechanical properties of the small component are very sensitive to geometries, and hence, it is important to test them properly in their actual dimensions and geometries.

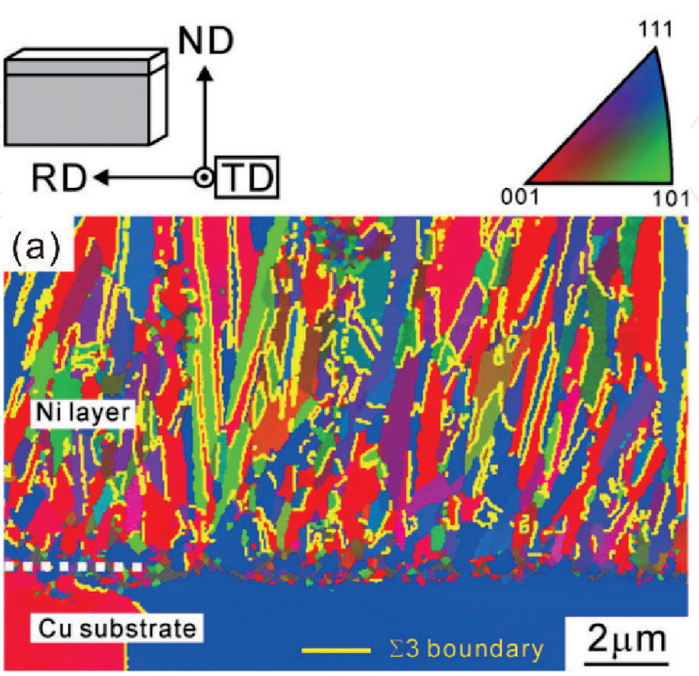

Figure 6.
Cross-sectional orientation map of nickel film. Yellow line delineates the Σ3 boundaries.

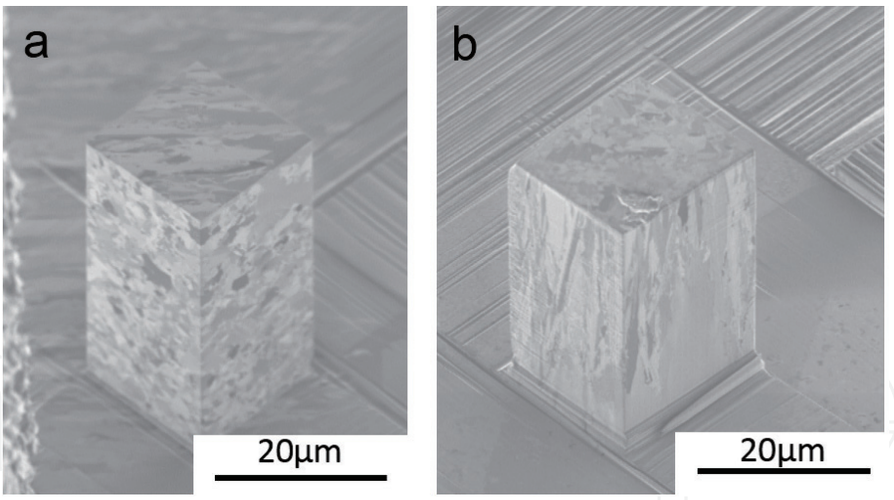

Figure 7.
Scanning ion microscopy images of fabricated compression pillar with growth direction (a) vertical and (b) parallel to the pillar axis.

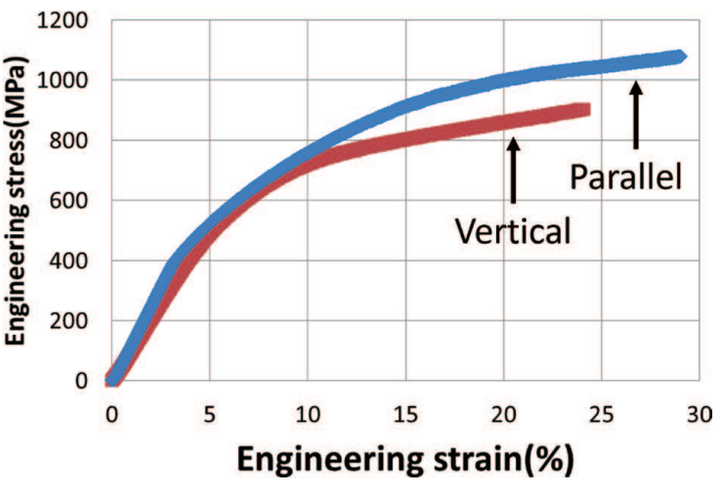

Figure 8.
Stress-strain curves of micro-compressions of vertical and parallel pillar.

2.3 Sample size effect on nanocrystalline nickel

The size effect known as the mechanical property changes by the varying sample size below; several tens of microns had been extensively studied as summarized in the introduction. However, the sample size effect on the nanocrystalline metals had been under controversy including the existence of it. On the other hand, nanocrystalline materials are very important for MEMS components, while the aforementioned structural or orientation anisotropy is usually not involved even in submicron-sized samples. Microcompressions of nanocrystalline nickel with a different sample size are conducted to evaluate sample size effect on nanocrystalline materials [39].

Nanocrystalline nickel was electrodeposited with the ESCE mentioned in the introduction, which was developed in our group. Emulsions were formed by stirring the electrolyte with polyoxyethylene lauryl ether ($C_{12}H_{25}(OCH_2CH_2)_{15}OH$) under high pressure (15 MPa) of supercritical carbon dioxide. Plated nanocrystalline nickel (NCNi) and single-crystal nickel (SCNi) purchased from Nilaco Inc. were used to fabricate compression pillars. Square cross-sectional pillars with side length ranging from 5 to 30 μm are fabricated. Micro-compression testing was conducted by custom-made testing machine with flat-ended diamond indenter with a strain rate of 2.5×10^{-3}.

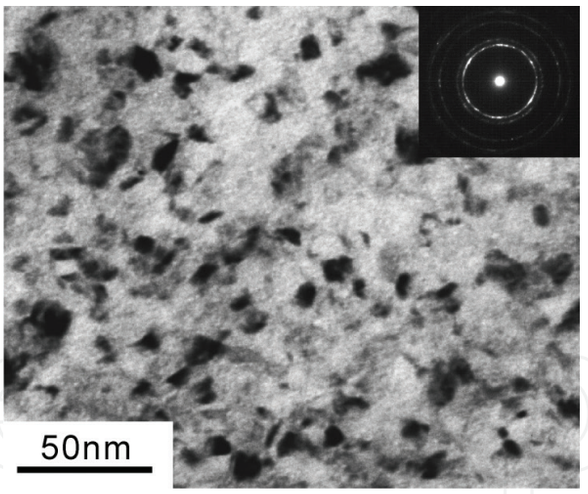

Figure 9.
TEM bright-field image of ESCE nickel viewed from film plane.

Deposited nanocrystalline nickel had 7.7 nm of average grain size measured by using TEM as shown in **Figure 9**. Pillars of SCNi with compression axis along <789> crystal orientation as analyzed by EBSD and NCNi were compression tested, and the results are shown in **Figure 10**. SCNi has a very low yield stress of 10–20 MPa which agrees well with the reported critical resolved shear stress of nickel. After yielding, large work hardening is due to the cross slip of dislocations, while several slip systems can be operative in compressions of near [111] orientation. And finally work is softened by the macroscopic shear formation. Compression tests of NCNi were shown in true plastic strain starting from 0.2% offset stress as yield stress, which is more than ten times higher than that of SCNi. The deformation process is believed to be a grain boundary process, such as grain boundary sliding or grain rotation.

1% flow stress and yield strength of NCNi and peak stress of SCNi, were plotted against the sample size in double logarithmic scale in **Figure 11**. The stress dependence on sample size was negative, which means the smaller one is stronger in both single crystal and nanocrystalline materials. Although the scaling exponent of −0.125 for NCNi was very small compared with SCNi, strength increased from 2.5 to 3.1 GPA when the pillar size was decreased from 30 to 5 μm. The size effect in the present NCNi can be considered as a result of grain boundary sliding, which is reported to involve several grains in formation of micro shear band along the grain boundaries known as cooperative grain boundary sliding (CGBS) [40]. CGBS events could initiate from flat segment of grain boundaries, and the number of these segments decreased when sample size becomes smaller. Increase in strength with decreased sample size is the consequence of decreased shear areas in the operation of CGBS.

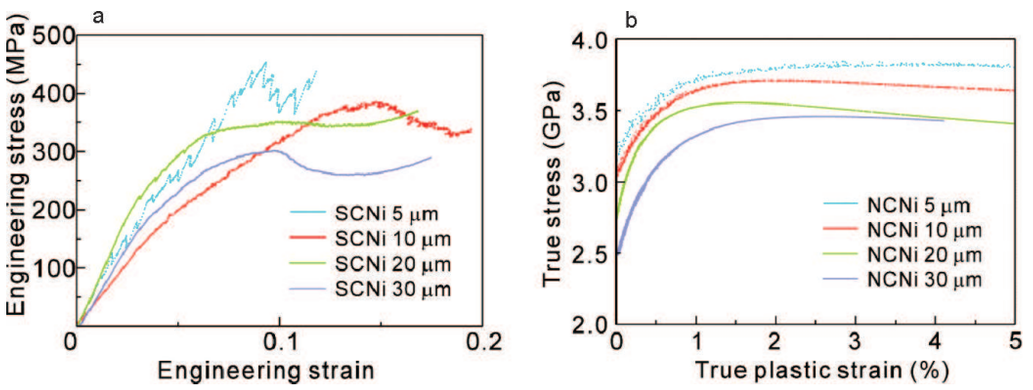

Figure 10.
Results of micro-compression test of sample with different sample sizes: (a) SCNi and (b) NCNi.

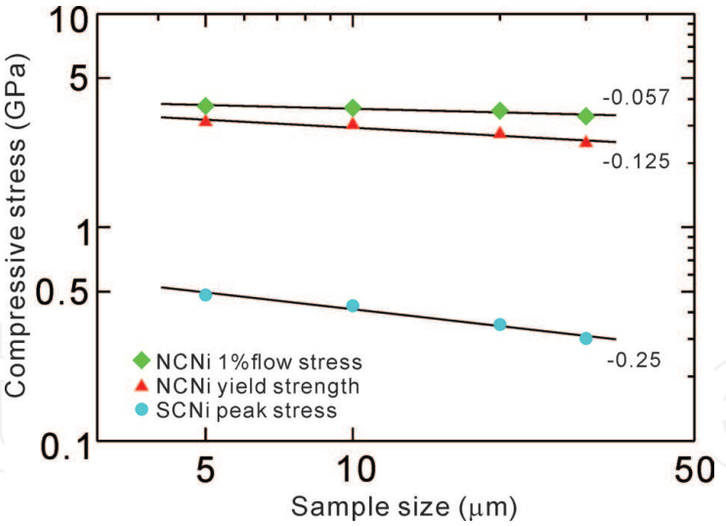

Figure 11.
Sample size dependence of compressive stresses.

3. Micro-tensile tests

3.1 Testing methods

Evaluating mechanical properties, such as fracture strength and elongation, of the materials in microscale is important to determine reliability of the micro-components used in MEMS. Although micro-compressions or micro-bending tests can provide some mechanical properties, these properties cannot be provided directly. For bulk materials, tensile tests are often used to evaluate mechanical properties including fracture strength and elongation and fracture behavior. Therefore, a tensile test in the microscale is needed to evaluate the properties of the micro-specimens. In the microscales, gripping the specimen and aligning the equipment for the tensile test are very difficult when comparing with micro-compression or bending tests; thus, there are only a few reports on micro-tensile test [41, 42]. The fabrication method of compression pillar shown in the previous section uses ion beam irradiation from vertical to pillar axis; thus, in a fabrication of tensile test specimen, the head of the sample and gauge part are separately fabricated as shown in **Figure 12**. At first, the thin sample was milled roughly by FIB, as shown in **Figure 12a**. Second, the grip part and gauge part were milled to a shape as shown in **Figure 12b**. Finally, the gauge part of the micro-tensile specimen was milled by the same way of the fabrication of compression pillar. The final shape of tensile specimen is shown in **Figure 12c**. High strength and stiffness of diamond are suitable materials for the micro-gripper to be used in micro-tensile test. Thus, the micro-gripper fabricated from the diamond-tip indenter can be used to evaluate mechanical property of high-strength materials.

Figure 12.
Schematics of tensile specimen fabrication. (a) Rough milling, (b) fabrication of grip part, and (c) SEM image of tensile specimen after gauge part milling by non-tapered pillar fabrication procedures.

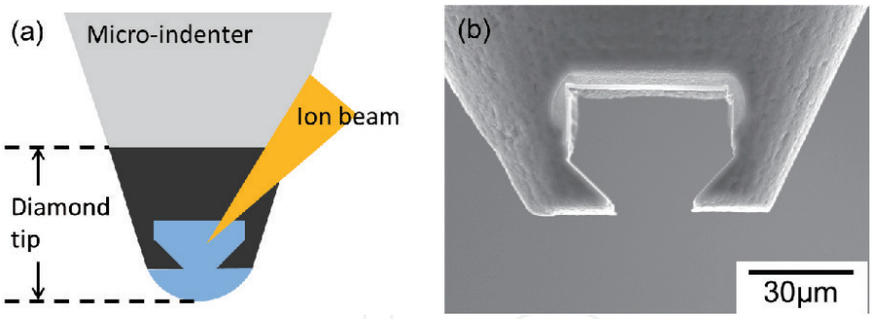

Figure 13.
Schematic image showing fabrication method of the micro-gripper for the micro-tensile test and (b) SEM image of the fabricated micro-gripper.

Using same FIB equipment for fabrications of grip part and sample gripper enables the completely inverted-shaped combination of them feasible for aligned grip in tensile test. The grip part of the micro-gripper was fabricated by removing away the blue region by FIB milling as shown in **Figure 13a**. **Figure 13b** shows SEM image of fabricated micro-gripper taken along the direction of FIB irradiation.

3.2 Tensile test of single-crystal nickel

Aside from the structural anisotropy on polycrystalline metals shown in the previous section, single-crystal metals have strong anisotropy to mechanical properties. We have conducted tensile test of SCNi with different orientations of <111> and <223> along loading axis [43]. The difference in the stress-strain curves shown in **Figure 14** is an evidence of the effect of crystal anisotropy on the deformation behavior. In particular, stress-strain curve of the <223> oriented specimen can be divided into three hardening stages as shown in dashed line in **Figure 14**. The three-stage hardening for <223> specimen is typically observed in single-crystal bulk metals with fcc structure [44]. The regions divided by the dashed lines are named stages 1, 2, and 3 from left to right, respectively. In stage 1, single slip system having a high Schmid factor easily glides at a low tensile strength. In stage 2, a multiple slip events occurred due to other glides in slip systems with lower Schmid factor than the one already worked in stage 1. Thus, the work hardening rate increased due to cutting and tangling of dislocation lines. In stage 3, the dislocation multiplication is limited due to the saturation of dislocations. Work hardening rate is decreased. However, the three-stage deformation behavior observed in <223> specimen was not observed in the <111> specimen. For the <111> specimen, a multiple slip phenomenon occurred at the initial region of plastic deformation, which is same as observed in stage 2 for the <223> specimen. The difference comes from that there is no slip system having a Schmid factor that is much larger than the others as the case in the <223> specimen. In addition, four slip systems had similar high Schmid factor which indicates they can move at similar stress on the contrary to <223> specimen. The behavior observed in the true-stress-true-strain curve for the <111> specimen is also similar to the stress-strain curve of bulk single-crystal metal composed of fcc crystal structure having multiple slip [44, 45]. Strength and deformation behavior of single-crystal metals are highly dependent on the loading directions even in the microscale tensile testing.

3.3 Tensile test of nanocrystalline nickel

The high strength and sample size effect on NCNi deposited by our developed method ESCE were evaluated by the micro-compression test. However,

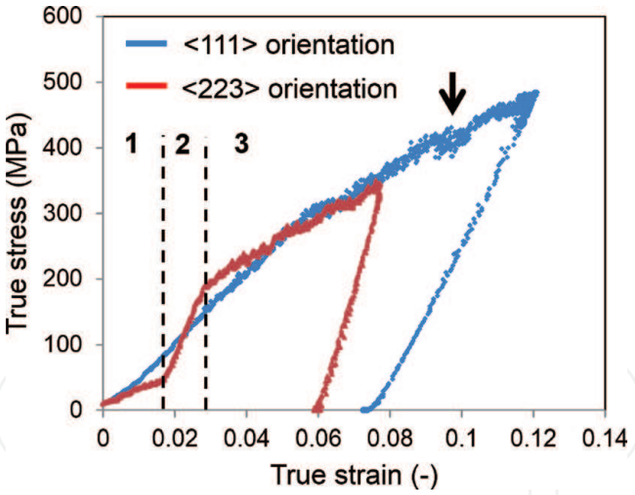

Figure 14.
Stress-strain curves of micro-tensile test conducted for single-crystal nickel oriented <111> and < 223> to loading axis.

micro-compression testing does not provide fracture strength and elongation to failure. The aim of tensile test conducted is to obtain these mechanical properties and to clarify underlying deformation mechanisms of nanocrystalline nickel [46].

Figure 15 shows engineering stress-strain curves of NCNi tested in micro-tensile test, sample A tensile loaded until fracture and sample B unloaded after maximum tensile stress was reached. Both samples had worked softening after plastic strains of 1% indicating almost no work hardening capacity. Observations of sample A and B are shown in **Figure 16**. In sample B, a notable necking was observed at the gauge part as shown in a magnified view in **Figure 16a**, and the rest of the portions was left undeformed. For nanocrystalline or ultrafine-grained materials with grain size smaller than 1 μm, these low work hardening capacities and the absence of uniform elongations are observed in tensile test using bulk specimen [47, 48]. The metals with small grains have no space for multiplication of dislocations during deformation; thus, dislocations immediately relaxed or sank in grain boundaries, and no dislocation hardening was attained. However, the fracture surface had shear lips at the edge of the specimen and dimples as shown in **Figure 16a** and **b** indicating the ductile nature of deformation. Testing by the different loading conditions reveals underlying the nature of deformation behavior important for the mechanical property analysis.

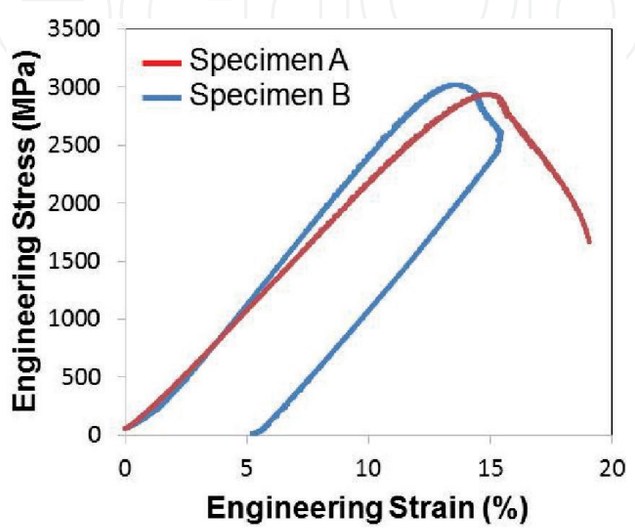

Figure 15.
Stress-strain curves of micro-tensile test conducted for ESCE nickel.

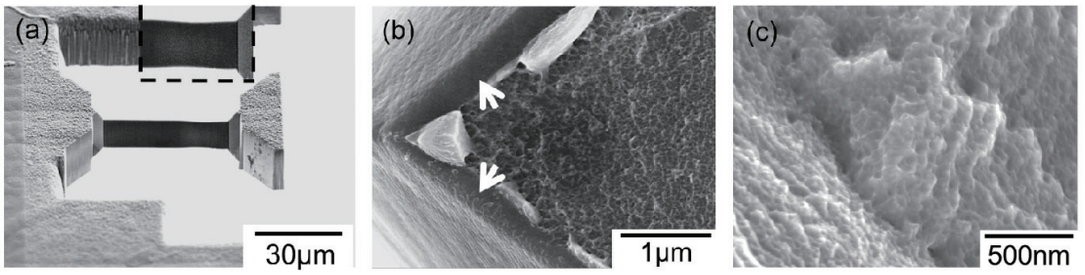

Figure 16.
SEM images of the specimen after micro-tensile test. (a) Specimen B, (b) shear lip observed on fractured surface of specimen A, and (c) dimple patterns on the center of fractured surface.

4. Conclusion

The present chapter describes a variety of micro-testing suitable for evaluations of mechanical properties of deposited films. Different geometries and loading directions are essential for the practical evaluations of mechanical properties of materials to be used in MEMS components. The sample preparation for micro-testing, our proposed fabrication method of microscale samples for compression and tension tests, demonstrated the anisotropic deformation behavior of electrodeposited metals.

Compression test conducted on nickel film deposited by conventional method, which has structural anisotropy as columnar grains grow along the deposition direction. The strength of the film is varied due to both geometry and loading directions indicating the importance of micro-testing the MEMS components with their actual dimensions.

Micro-compression and tensile test reveal very high strength and peculiar deformation behavior of nanocrystalline nickel deposited in ESCE. And more importantly, the size effect on nanocrystalline materials has been observed and concluded to be due to the decreased shear areas of CGBS in small samples.

Author details

Takashi Nagoshi[1*], Tso-Fu Mark Chang[2]

1 National Institute of Advanced Industrial Science and Technology, Tsukuba, Japan

2 Tokyo Institute of Technology, Yokohama, Japan

*Address all correspondence to: nagoshi-t@aist.go.jp

References

[1] Giomi E, Fanucci L, Rocchi A. Analog-CMDA based interfaces for MEMS gyroscopes. Microelectronics Journal. 2014;**43**:78-88

[2] Oliver WC, Pharr GM. Improved technique for determining hardness and elastic modulus using loading and displacement sensing indentation. Journal of Materials Research. 1992;**7**:1564-1580

[3] Ma Q, Clarke DR. Size dependent hardness in silver single crystals. Journal of Materials Research. 1995;**10**:853-863

[4] Nix WD, Gao H. Indentation size effects in crystalline materials: A law for strain gradient plasticity. Journal of the Mechanics and Physics of Solids. 1998;**46**:411-425

[5] Ashby MF. The deformation of plastically non-homogeneous materials. Philosophical Magazine. 1970;**21**:399-424

[6] Dimiduk DM, Uchic MD, Parthasarathy TA. Size-affected single-slip behavior of pure nickel microcrystals. Acta Materialia. 2005;**53**:4065

[7] Frick CP, Clark BG, Orso S, Schneider AS, Arzt E. Size effect on strength and strain hardening of small-scale [1 1 1] nickel compression pillars. Materials Science and Engineering A. 2008;**489**:319

[8] Greer JR, Oliver WC, Nix WD. Size dependence of mechanical properties of gold at the micron scale in the absence of strain gradients. Acta Materialia. 2005;**53**:1821

[9] Volkert CA, Lilleodden ET. Size effects in the deformation of sub-micron Au columns. Philosophical Magazine. 2006;**86**:5567

[10] Kiener D, Motz C, Dehm G. Micro-compression testing: A critical discussion of experimental constraints. Materials Science and Engineering A. 2009;**505**:79

[11] Ng KS, Ngan AHW. Deformation of micron-sized aluminium bi-crystal pillars. Acta Materialia. 2008;**56**:1712

[12] Greer JR, Nix WD. Nanoscale gold pillars strengthened through dislocation starvation. Physical Review B. 2006;**73**:245410

[13] Parthasarathy TA, Rao SI, Dimiduk DM, Uchic MD, Trinkle DR. Contribution to size effect of yield strength from the stochastics of dislocation source lengths in finite samples. Scripta Materialia. 2007;**56**:313-316

[14] Beanland R. Dislocation multiplication mechanisms in low-misfit strained epitaxial layers. Journal of Applied Physics. 1995;**77**:6217-6222

[15] Hemker KJ, Nix WD. Nanoscale deformation: Seeing is believing. Nature Materials. 2008;**7**:97-98

[16] Oh SH, Legros M, Kiener D, Dehm G. In situ observation of dislocation nucleation and escape in a submicrometre aluminium single crystal. Nature Materials. 2009;**8**:95-100

[17] Cui YN, Lin P, Liu ZL, Zhuang Z. Theoretical and numerical investigations of single arm dislocation source controlled plastic flow in FCC micropillars. International Journal of Plasticity. 2014;**55**:279-292

[18] Schiøtz J, Tolla FDD, Jacobsen KW. Softening of nanocrystalline metals at very small grain sizes. Nature. 1998;**391**:561

[19] Rinaldi A, Peralta P, Friesen C, Sieradzki K. Sample size-effects in the yield behavior of nanocrystalline Ni. Acta Materialia. 2008;**56**:511

[20] Jang D, Greer JR. Size-induced weakening and grain boundary-assisted deformation in 60 nm grained Ni nanopillars. Scripta Materialia. 2011;**64**:77-80

[21] Sun Y, Miyasato T, Wigmore JK, Sonoda N, Watari Y. Characterization of 3C-SiC films grown on monocrystalline Si by reactive hydrogen plasma sputtering. Journal of Applied Physics. 1997;**82**:2334

[22] Yoshida T, Tani T, Nishimura H, Akashi K. Characterization of a hybrid plasma and its application to a chemical synthesis. Journal of Applied Physics. 1983;**54**:640

[23] Gad-el-Hak M. The MEMS Handbook. Boca Raton, FL: CRC, Taylor & Francis; 2006

[24] Schultze JW, Bressel A. Principles of electrochemical micro- and nano-system technologies. Electrochimica Acta. 2001;**47**:3

[25] Tsai WL, Hsu PC, Hwu Y, Chen CH, Chang LW, Je JH, et al. Electrochemistry: Building on bubbles in metal electrodeposition. Nature. 2002;**417**:139

[26] Yoshida H, Sone M, Wakabayashi H, Yan H, Abe K, Tao XT, et al. New electroplating method of nickel in emulsion of supercritical carbon dioxide and electrolyte solution to enhance uniformity and hardness of plated film. Thin Solid Films. 2004;**446**:194

[27] Yan H, Sone M, Sato N, Ichihara S, Miyata S. The effects of dense carbon dioxide on nickel plating using emulsion of carbon dioxide in electroplating solution. Surface and Coating Technology. 2004;**182**:329

[28] Yoshida H, Sone M, Mizushima A, Yan H, Wakabayashi H, Abe K, et al. Application of emulsion of dense carbon dioxide in electroplating solution with nonionic surfactants for nickel electroplating. Surface and Coating Technology. 2003;**173**:285

[29] Chang TFM, Sone M, Shibata A, Ishiyama C, Higo Y. Bright nickel deposited by supercritical carbon dioxide emulsion using additive-free Watts bath. Electrochimica Acta. 2010;**55**:6469

[30] Shinoda N, Shimizu T, Chang TFM, Shibata A, Sone M. Filling of nanoscale holes with high aspect ratio by Cu electroplating using suspension of supercritical carbon dioxide in electrolyte with Cu particles. Microelectronic Engineering. 2012;**97C**:126

[31] Shimizu T, Ishimoto Y, Chang TFM, Kinashi H, Nagoshi T, Sato T, et al. Cu wiring into nano-scale holes by electrodeposition in supercritical carbon dioxide emulsified electrolyte with a continuous flow reaction system. Journal of Supercritical Fluids. 2014;**60**:60

[32] Uchic MD, Dimiduk DM, Florando JN, Nix WD. Sample dimensions influence strength and crystal plasticity. Science. 2004;**305**: 986-989

[33] Zhang H, Schuster BE, Wei Q, Ramesh KT. The design of accurate micro-compression experiments. Scripta Materialia. 2006;**54**:181-186

[34] Humphreys FJ, Hartherly M. Recrystallization and Related Annealing Phenomena. 2nd ed. Amsterdam: Elsevier; 2004

[35] Nakahara S. Growth twins and development of polycrystallinity in electrodeposits. Journal of Crystal Growth. 1981;**55**:281

[36] Bastos A, Zaefferer S, Raabe D, Schuh C. Characterization of the microstructure and texture of

nanostructured electrodeposited NiCo using electron backscatter diffraction (EBSD). Acta Materialia. 2006;**54**:2451

[37] Shinada E, Nagoshi T, Chang TFM, Sone M. Crystallographic study on self-annealing of electroplated copper at room temperature. Materials Science in Semiconductor Processing. 2013;**16**:633

[38] Imamura H, Nagoshi T, Yoshida A, Chang TFM, Onaka S, Sone M. Evaluation of anisotropic structure in electrodeposited Ni film using micro-sized cantilever. Microelectronic Engineering. 2012;**100**:25

[39] Nagoshi T, Mutoh M, Chang TFM, Sato T, Sone M. Sample size effect of electrodeposited nickel with sub-10 nm grain size. Materials Letters. 2014;**117**:256-259

[40] Zelin MG, Mukherjee AK. Cooperative phenomena at grain boundaries during superplastic flow. Acta Metallurgica et Materialia. 1995;**43**:2359

[41] Haque MA, Saif MTA. A review of MEMS-based microscale and nanoscale tensile and bending testing. Experimental Mechanics. 2003;**43**:248

[42] Kiener D, Grosinger W, Dehm G, Pippan R. A further step towards an understanding of size-dependent crystal plasticity: In situ tension experiments of miniaturized single-crystal copper samples. Acta Materialia. 2008;**56**:580-592

[43] Kihara Y, Nagoshi T, Chang TFM, Hosoda H, Sato T, Sone M. Tensile behavior of micro-sized specimen made of single crystalline nickel. Materials Letters. 2015;**153**:36-39

[44] Honeycombe RWK. The Plastic Deformation of Metals. 2nd ed. London: Butler & Tanner Ltd; 1984

[45] Cottrell AH. Dislocations and Plastic Flow in Crystals. Oxford: Clarendon Press; 1953

[46] Kihara Y, Nagoshi T, Chang TFM, Hosoda H, Sato T, Sone M. Tensile behavior of micro-sized specimen fabricated from nanocrystalline nickel film. Microelectronic Engineering. 2015;**141**:17-20

[47] Wang YM, Ma E. Three strategies to achieve uniform tensile deformation in a nanostructured metal. Acta Materialia. 2004;**52**:1699-1709

[48] Torre FD, Swygenhoven HV, Victoria M. Nanocrystalline electrodeposited Ni: Microstructure and tensile properties. Acta Materialia. 2002;**50**:3957-3970